Ultrasound in Med. & Biol., Vol. 40, No. 6, pp. 1379–1384, 2014

0301-5629/$ - see front matter

http://dx.doi.org/10.1016/j.ultrasmedbio.2013.11.025

● *Technical Note*

ON THE ACOUSTIC PROPERTIES OF VAPORIZED SUBMICRON PERFLUOROCARBON DROPLETS

Nikita Reznik,* Guillaume Lajoinie,† Oleksandr Shpak,† Erik C. Gelderblom,† Ross Williams,‡ Nico de Jong,§ Michel Versluis,† and Peter N. Burns*‡

*Department of Medical Biophysics, University of Toronto, Toronto, Ontario, Canada; †Physics of Fluids Group and MIRA Institute of Biomedical Technology and Technical Medicine, University of Twente, Enschede, The Netherlands; ‡Sunnybrook Research Institute, Toronto, Ontario, Canada; and §Biomedical Engineering Thoraxcenter, Erasmus Medical Center, Rotterdam, The Netherlands

(*Received* 23 *August* 2013; *revised* 19 *November* 2013; *in final form* 20 *November* 2013)

Abstract—The acoustic characteristics of microbubbles created from vaporized submicron perfluorocarbon droplets with fluorosurfactant coating are examined. Utilizing ultra-high-speed optical imaging, the acoustic response of individual microbubbles to low-intensity diagnostic ultrasound was observed on clinically relevant time scales of hundreds of milliseconds after vaporization. It was found that the vaporized droplets oscillate non-linearly and exhibit a resonant bubble size shift and increased damping relative to uncoated gas bubbles due to the presence of coating material. Unlike the commercially available lipid-coated ultrasound contrast agents, which may exhibit compression-only behavior, vaporized droplets may exhibit expansion-dominated oscillations. It was further observed that the non-linearity of the acoustic response of the bubbles was comparable to that of SonoVue microbubbles. These results suggest that vaporized submicron perfluorocarbon droplets possess the acoustic characteristics necessary for their potential use as ultrasound contrast agents in clinical practice. (E-mail: reznik@ohsu.edu) **© 2014 World Federation for Ultrasound in Medicine & Biology.**

Key Words: **Ultrasound contrast agents, Perfluorocarbon droplets, Droplet vaporization, High-speed imaging, Microbubble characterization.**

INTRODUCTION

Contrast-enhanced ultrasound is a well-established diagnostic imaging technique. Microbubble ultrasound contrast agents are small, encapsulated spheres of gas, typically 1 to 5 μm in diameter. Their size, similar to that of red blood cells, makes them a true blood pool agent, allowing for their use in a number of diagnostic applications, such as cancer detection (Burns and Wilson 2007), assessment of blood flow (Hudson et al. 2011) and blood pressure measurements (Tremblay-Darveau et al. 2014). However, their size is also a disadvantage for some applications, as microbubbles are confined to the blood vessels and cannot reach extravascular targets.

Submicron droplets of liquid perfluorocarbon (PFC) have been studied as a new generation of extravascular contrast agents for ultrasound. At a size of a few hundreds of nanometers in diameter, these droplets have the ability to extravasate selectively in regions of tumor growth and stay intravascular in healthy tissues, due to the enhanced permeability and retention effect (Maeda et al. 2000), effectively allowing for their passive targeting to tumors. The low-boiling-point droplets are acoustically inert, until exposed to a sufficiently high-intensity burst of ultrasound, at which point they vaporize to produce echogenic microbubbles (Reznik et al. 2011), stabilized by the coating material used to encapsulate their liquid droplet precursors for time scales of seconds to minutes (Reznik et al. 2012). Such extravascular contrast agents may be used for diagnostic ultrasound imaging to detect regions of tumor growth (Matsunaga et al. 2012; Williams et al. 2013) as well as for therapeutic applications, such as sensitizers for high-intensity focused ultrasound (HIFU) therapy (Phillips et al. 2013) and vehicles for drug delivery (Rapoport 2012).

For their successful application as ultrasound contrast agents (UCAs), upon vaporization, the droplets should produce echogenic bubbles that respond to ultrasound in a manner similar to the currently used microbubbles on

Address correspondence to: Nikita Reznik, Knight Cardiovascular Institute, Oregon Health & Science University, 3181 SW Sam Jackson Road, UHN62, Portland, OR 97239, USA. E-mail: reznik@ohsu.edu

clinically relevant time scales of hundreds of milliseconds. Although a number of studies have focused on the conditions necessary for droplet nucleation (Couture et al. 2012; Kripfgans et al. 2000; Reznik et al. 2011; Sheeran et al. 2011; Shpak et al. 2013a; Williams et al. 2013) and the vaporization process itself (Reznik et al. 2013; Sheeran et al. 2013; Shpak, et al. 2013b; Sheeran et al. 2014), only limited information is available regarding the acoustic properties of these newly created microbubbles.

In this report we conduct an initial study of the acoustic properties of individual vaporized PFC droplets. Using ultra-high-frame rate optical imaging, we examine the acoustic response of the fully vaporized microbubbles of different sizes to a 2.5-MHz ultrasound pulse of low intensity (mechanical index [MI] < 0.1) a few hundreds of milliseconds after the phase change. Specifically, we examine the change in bubble oscillation amplitude and non-linearity of oscillation as a function of bubble size. Furthermore, we study the influence of the presence of coating material on bubble oscillations and compare the non-linear acoustic response of these bubbles with that of commercially available SonoVue microbubbles, to assess whether the vaporized droplets possess adequate acoustic properties for their potential use as UCAs.

METHODS

Droplet preparation

Perfluorocarbon droplet emulsions were prepared by combining water, 5% v/v dodecafluoropentane (PFP, Fluoromed, Round Rock, TX, USA) and 0.8% v/v negatively charged fluorosurfactant Zonyl FSP (Sigma Aldrich, St. Louis, MO, USA) according to a previously established protocol (Reznik et al. 2013). The samples were coarse emulsified with a Vortex mixer (VM-300, Gemmy Industrial, Cherry Hill, NJ, USA) for 30 s. After the coarse emulsification, the solution was further emulsified with a tip sonicator (Sonifier 250, Branson, Branson, MO, USA) for 60 s at 80% duty cycle. Sizing of the droplets was performed with a Zetasizer nano-sizing system (Malvern, Worcestershire, UK). This method provided droplet samples that were polydispersed in size, ranging from 100 nm to 1 μm in diameter, with mean diameter of approximately 400 nm.

Droplet vaporization

A schematic of the experimental setup used for droplet vaporization and bubble characterization studies is provided in Figure 1. Both the high-intensity vaporization pulse and the low-intensity characterization pulses were sent from a 5-MHz-center-frequency Olympus transducer (A308S, Olympus, Quebec City, QC, Canada), driven by an arbitrary waveform generator (8026, Tabor, Tel Hanan, Israel) amplified by an E&I 350L (E&I, Rochester, NY, USA) power amplifier. The transducer output was calibrated with a 0.2-mm needle hydrophone probe (Precision Acoustics, Dorchester, UK). The transducer was focused on an Opticell containing the droplet sample. The droplet sample consisted of the originally prepared droplet solution, diluted 1:2000 in distilled water and degassed with a vacuum pump for at least 1 h. The Opticell was placed under a 60× water-immersion objective (NA = 1.00) of an Olympus BX-FM microscope, coupled to the Brandaris 128 ultra-high speed imaging system (Chin et al. 2003), providing a spatial resolution of 160 nm/pixel. The microscope objective was co-aligned with the transducer focus. The focal point was 50 μm above the wall of the Opticell, such that wall proximity would not have a significant effect on subsequent bubble oscillation (Garbin et al. 2007). The setup was placed in a tank filled with de-ionized water kept at a temperature of 37 ± 1°C. Droplet samples were vaporized with single ultrasound pulses, 10 cycles in length, and a peak negative pressure (PNP) of 3.5 MPa.

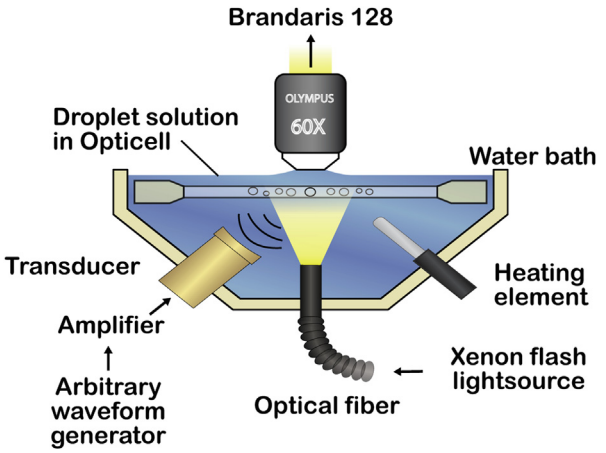

Fig. 1. Schematic diagram of the experimental setup. Acoustic high-intensity vaporization and low-intensity characterization pulses were sent from the single-element transducer. Detection was accomplished using a 60× objective of an Olympus microscope.

Vaporized droplet characterization experiment

After vaporization, a series of five low-intensity acoustic characterization pulses were sent. The pulses were 10 cycles in length, 2.5 MHz in center frequency and 116 kPa in PNP, corresponding to an MI of 0.07. The pulses were sent either 80 or 100 ms apart. As a result, the bubbles were observed at times ranging from 80 to 500 ms after vaporization, based on the pulse timing interval used for the specific trial. Bubble oscillations in response to the acoustic pulses were recorded optically in a series of movies of 128 frames each, recorded at 15 million frames per second (Mfps). For our analysis, we

considered only recordings that depicted bubbles in focus, such that their size and radial oscillations could be resolved with confidence. Furthermore, only images that contained either a single bubble or bubbles sufficiently far away from each other (at least 50 μs apart) were considered, to minimize the possible coupled oscillation effects (Allen et al. 2003; Garbin et al. 2009; Kokhuis et al. 2013).

Optical image analysis

Bubble contours from the recorded optical images were traced using an algorithm based on the minimum cost function (van der Meer et al. 2007), implemented in MATLAB (The MathWorks, Natick, MA, USA). The bubble radius was calculated as the mean distance from the bubble center of mass to the edge of the bubble in a radial coordinate system. This approach provided the radius-time (R–t) curves of the bubble response to acoustic characterization pulses. In total, 30 bubble traces were analyzed.

The acoustic pressure scattered by bubble oscillation has been calculated from the R–t curves using (Sijl et al. 2011b):

$$P_s(r,t) = \frac{\rho}{r}\left(R(t)^2\ddot{R}(t) + 2R(t)\dot{R}(t)^2\right) \qquad (1)$$

where P_S is the scattered acoustic pressure, ρ is the water density, r is the distance from the bubble surface, R is the bubble radius and the overdots denote derivatives with respect to time.

The scattered pressure traces calculated from eqn (1) in the time domain were Fourier transformed, and the integrated powers in the frequency bands of $\pm$300 kHz around the fundamental (2.5 MHz, f_1) and the second harmonic (5 MHz, f_2) were measured.

The experimental results were compared with numerical simulations for an uncoated bubble using a Rayleigh-Plesset-type equation. Furthermore, the results were also compared with those modeled by the de Jong model for coated microbubbles (de Jong et al. 1994), with shell stiffness S_p = 0.3 N/m and shell friction $S_f = 3.17 \times 10^{-7}$ kg/s, identified as best-fit parameters based on the oscillation amplitude results from the examined bubble traces.

RESULTS

Vaporization of suspensions of submicron PFC droplets produced microbubbles ranging in size from 500 nm to 5 μm in radius, which were stable on the clinically relevant time scales of hundreds of milliseconds. Oscillation of these newly created bubbles under low-intensity diagnostic ultrasound pulses has been successfully recorded by our imaging setup. Bubble traces were examined in both the time and frequency domains, as illustrated in the example of a 1.7-μm bubble oscillation in Figure 2. The experimentally observed trace appears to fit the de Jong model well and exhibits an oscillation amplitude substantially lower than that expected for an uncoated bubble (Fig. 2a). The power spectrum calculated from the R–t curve (Fig. 2b) depicts clear peaks around the fundamental frequency (2.5 MHz) and the second harmonic (5 MHz), evidence of a significant non-linear component in the bubble oscillation. None of the analyzed traces contained any observable subharmonic component.

Amplitude of oscillation

The total amplitude of bubble oscillations was measured from the maximum compression and expansion phases of the bubble, normalized to the resting radius. The Amplitude is plotted as a function of bubble size in Figure 3. Although there is a degree of variability, the experimental results appear to correspond to the response simulated using the de Jong model. There was an experimentally observed resting bubble radius of R_{res} = 1.75 μm, for which the bubble oscillation amplitude was at maximum. This resting radius is in concordance with that simulated by the de Jong model and significantly different from that of an uncoated bubble of R_0 = 1.3 μm. The measured amplitude of bubble oscillation is also in agreement with the results simulated by the de Jong model, and is substantially lower than that exhibited by the simulated uncoated bubble response.

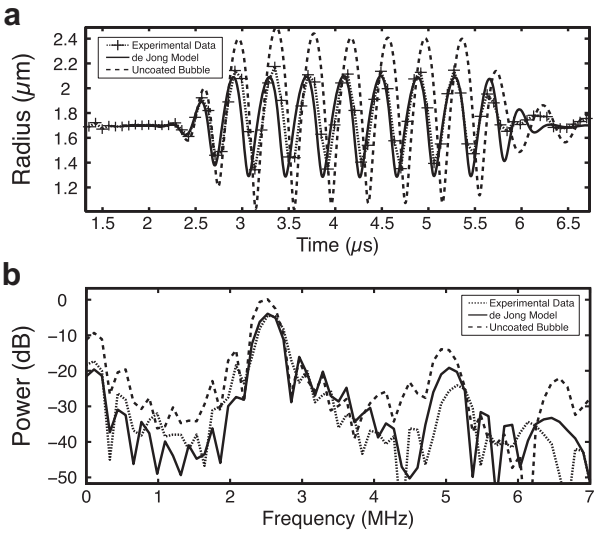

Fig. 2. (a) Radius-time trace of a bubble with initial radius of R_0 = 1.7 μm, with a fit by the de Jong model and the trace simulated for an uncoated bubble for the same size. (b) Frequency spectrum of the bubble oscillation, as calculated from the observed radius-time curve, together with the de Jong model fit and the spectrum obtained from simulated uncoated bubble oscillation.

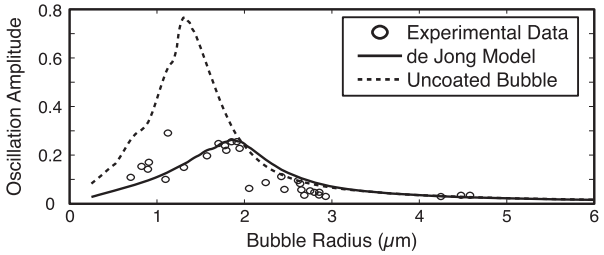

Fig. 3. Amplitude of bubble oscillation normalized to the bubbles' resting radii, as a function of the bubbles' resting radii. Shown are the experimental data, the best fit of the de Jong model and the simulated response from an uncoated bubble. A decrease in amplitude of oscillation and increase in resonant bubble size for the experimental results compared with the uncoated bubble simulation is apparent.

Furthermore, it was observed that the bubbles did not always oscillate symmetrically. The smaller bubbles, with radii below R_{res}, preferred expansion-dominated oscillations. At the same time, bubbles larger than approximately 2 μm in radius exhibited largely symmetric oscillations.

Non-linearity of emitted pressures

To assess the non-linearity in the emitted acoustic signal from the bubbles, pressure-time curves were calculated from the experimentally observed and the simulated *R–t* plots and analyzed in the frequency domain. To examine the degree of non-linearity, the integrated powers in the fundamental and second harmonic bands were calculated separately as a function of bubble size, as illustrated in Figure 4. The de Jong model appears to describe the bubble oscillation in the fundamental band and the general magnitude of the power of the second harmonic band. The ratio of the power in the second harmonic band to the power in the fundamental band was on the order of –5 to –15 dB, depending on bubble size.

DISCUSSION

Bubble acoustic behavior

In this work we look at the acoustic response of microbubbles created from their liquid droplet precursors at times ranging from 80 to 500 ms after vaporization. It is envisioned that the time scales of hundreds of milliseconds are the most relevant clinically as they are on the same order as the inter-frame times of typical clinical US scanners (operating at tens of hertz frame rates). The MI of the ultrasound characterization pulse used here (MI = 0.07) is lower than the typical MI of diagnostic ultrasound used in the clinic. However, the lower ultrasound pressure settings minimized the possibility of bubble cavitation or gas loss and other deflation effects, while allowing for the study of associated non-linear oscillation behavior of the bubbles.

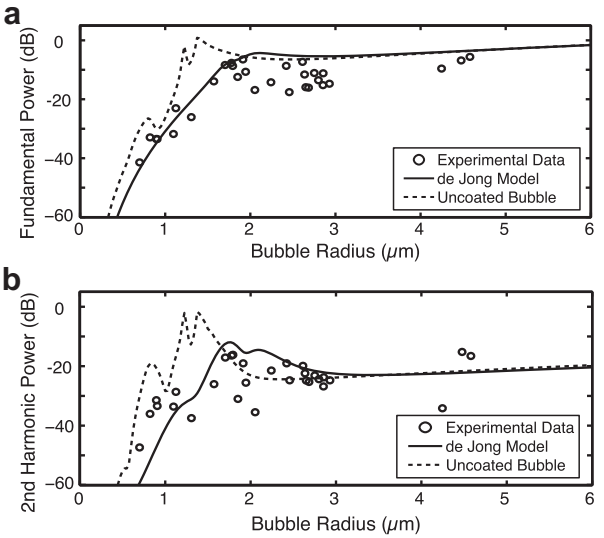

Fig. 4. Measured power of scattered acoustic pressure in the (a) fundamental and (b) second harmonic bands for experimentally obtained data and the simulated model results. The ratio of power in the second harmonic band to that in the fundamental band ranges from −5 to −15 dB.

Although the observed acoustic response of the bubbles has a significant degree of variability, general trends that can help assess the acoustic response of the vaporized PFC droplets for their potential application as UCAs are visible. For the characterization pulse used (2.5 MHz, 116 kPa PNP), there is a bubble radius of R_{res} = 1.75 μm associated with maximum bubble oscillation amplitude (Fig. 3). For simplicity, we refer to R_{res} as the resonant size. However, it is important to note that at the pressures investigated here, the bubbles exhibited a non-linear response, and the size of maximum oscillation R_{res} in this case may be significantly different from the resonant size of the bubble in the linear regime (Overvelde et al. 2010). The bubble resonant size is larger than that expected for an uncoated bubble, whereas the amplitude of bubble oscillation is lower than that of an uncoated bubble. A shift in R_{res} and decrease in oscillation amplitude are characteristic of the presence of a viscoelastic shell material. It has been reported previously (Reznik et al. 2012) that after vaporization, the newly created bubbles retain the original shell material stabilizing the droplet precursors. The results of the present study suggest that the surfactant coating originally on the droplets affects the acoustic behavior of the newly created microbubbles.

Simulated bubble response using the de Jong model describes the experimentally observed trends. The fitted shell elasticity parameter of S_p = 0.3 N/m is substantially lower than the measured value for clinically used SonoVue microbubbles of S_p = 1.1 N/m; however, the fitted

viscosity parameter of $S_f = 3.17 \times 10^{-7}$ kg/s appears to be similar to that of SonoVue (Gorce et al. 2000).

For the ultrasound pulses used here, vaporized PFC droplets do not appear to exhibit the characteristic "compression-only" behavior observed in some cases for lipid-coated microbubbles (Sijl et al. 2011a). On the contrary, bubbles smaller than the resonant size exhibit an expansion-dominated behavior, indicative of higher resistance to compression than expansion.

Suitability of vaporized PFC droplets for the role of UCAs

To assess the applicability of vaporized PFC droplets as UCAs, it is instructive to compare the observed bubble response with the previously studied acoustic responses from clinically used microbubbles, such as SonoVue. It has been found that smaller SonoVue microbubbles favor compression-dominated oscillations or even compression-only behavior because of the buckling of the lipid bubble shells (de Jong et al. 2007; Emmer et al. 2007). This comes in sharp contrast with the observed behavior of bubbles under consideration in this study that show a preference for expansion-dominated behavior. The lack of compression-dominated oscillations and no detectable sub-harmonic signal suggests that unlike the commercially available lipid-coated UCAs, vaporized fluorosurfactant-coated droplets under study do not exhibit shell buckling behavior, even at the relatively high oscillation amplitudes of up to 25% of the bubble radius.

At the same time, for the purposes of their application as UCAs, the non-linearity of the scattered pressure caused by bubble oscillation is paramount, as non-linear scattering serves as the basis for contrast-specific US imaging techniques, such as pulse-inversion imaging (Simpson et al. 1999). From the experimentally observed data, the ratio of scattered acoustic signal powers in the second harmonic band to fundamental band is on the order of −5 to −15 dB (Fig. 4) for US at a frequency of 2.5 MHz and MI of 0.07. These values are similar to the value of approximately −12 dB observed for SonoVue microbubble populations (Schneider 1999) at the same MI for a 2.25 MHz excitation frequency. It should, however, be noted that the results of this study for vaporized droplets were obtained by optical observation of single bubbles, whereas the characterization results for SonoVue in the referenced works (Gorce et al. 2000; Schneider 1999) were obtained by an acoustic interrogation of bubble populations. Thus, only a qualitative comparison can be done. Although there is similarity in the acoustic responses of the two types of bubbles, more detailed and controlled examinations are necessary to quantitatively compare the two. The results presented here indicate that, on clinically relevant time scales, the acoustic response of vaporized droplets is similar to that of clinically used microbubble agents and supports their future utilization as UCAs.

CONCLUSIONS

The work described here investigated the acoustic characteristics of vaporized submicron droplets on clinically relevant time scales. It was found that after vaporization with ultrasound, the newly created microbubbles oscillate non-linearly and exhibit coating material-induced effects on oscillation that can be described by the de Jong coated bubble dynamics model. The coating material on the surface of the bubbles induces a shift in the resonance frequency and a substantial amount of damping because of shell viscosity.

Unlike lipid-coated UCAs, the fluorosurfactant-coated bubbles used in this study do not exhibit buckling behavior, and tend to feature expansion-dominated oscillations for smaller bubbles. At the same time, it was found that vaporized PFC droplets scatter ultrasound in a manner similar to that of the currently clinically used microbubble contrast agents. These results suggest that stable vaporized PFC droplets possess the adequate acoustic characteristics to support their potential use as UCAs in the clinic.

Acknowledgments—This work was supported by the Ontario Institute of Cancer Research, the Natural Sciences and Engineering Research Council of Canada and the Canadian Institutes of Health Research. This work is also part of the research program of the Foundation for Fundamental Research on Matter (FOM), which is financially supported by the Netherlands Organization for Scientific Research (NWO).

REFERENCES

Allen JS, Kruse DE, Dayton PA, Ferrara KW. Effect of coupled oscillations on microbubble behavior. J Acoust Soc Am 2003;114:1678–1690.

Burns PN, Wilson SR. Focal liver masses: Enhancement patterns on contrast-enhanced images—Concordance of US scans with CT scans and MR images. Radiology 2007;242:162–174.

Chin CT, Lancée C, Borsboom JMG, Mastik F, Frijlink ME, de Jong N, Versluis M, Lohse D. Brandaris 128: A digital 25 million frames per second camera with 128 highly sensitive frames. Rev Sci Instrum 2003;74:5026–5034.

Couture O, Urban A, Bretagne A, Martinez L, Tanter M, Tabeling P. In vivo targeted delivery of large payloads with an ultrasound clinical scanner. Med Phys 2012;39:5229–5237.

De Jong N, Cornet R, Lancee C. Higher harmonics of vibrating gas-filled microspheres: 1. Simulations. Ultrasonics 1994;32:447–453.

De Jong N, Emmer M, Chin CT, Bouakaz A, Mastik F, Lohse D, Versluis M. 'Compression-only' behavior of phospholipid-coated contrast bubbles. Ultrasound Med Biol 2007;33:653–656.

Emmer M, van Wamel A, Goertz DE, de Jong N. The onset of microbubble vibration. Ultrasound Med Biol 2007;33:941–949.

Garbin V, Cojoc D, Ferrari E, Di Fabrizio E, Overvelde MLJ, van der Meer SM, de Jong N, Lohse D, Versluis M. Changes in microbubble dynamics near a boundary revealed by combined optical micromanipulation and high-speed imaging. Appl Phys Lett 2007;90:114103.

Garbin V, Dollet B, Overvelde MLJ, Cojoc D, Di Fabrizio E, van Wijngaarden L, Prosperetti A, de Jong N, Lohse D, Versluis M. History force on coated microbubbles propelled by ultrasound. Phys Fluids 2009;21:092003.

Gorce JM, Arditi M, Schneider M. Influence of bubble size distribution on the echogenicity of ultrasound contrast agents: A study of SonoVue. Invest Radiol 2000;35:661–671.

Hudson JM, Williams R, Lloyd B, Atri M, Kim TK, Bjarnason GA, Burns PN. Improved flow measurement using microbubble contrast agents and disruption-replenishment: clinical application to tumour monitoring. Ultrasound Med Biol 2011;37:1210–1221.

Kokhuis TJA, Garbin V, Kooiman K, Naaijkens BA, Juffermans LJM, Kamp O, van der Steen AFW, Versluis M, de Jong N. Secondary Bjerknes forces deform targeted microbubbles. Ultrasound Med Biol 2013;39:490–506.

Kripfgans OD, Fowlkes JB, Miller DL, Eldevik OP, Carson PL. Acoustic droplet vaporization for therapeutic and diagnostic applications. Ultrasound Med Biol 2000;26:1177–1189.

Maeda H, Wu J, Sawa T, Matsumura Y, Hori K. Tumor vascular permeability and the EPR effect in macromolecular therapeutics: A review. J Control Release 2000;65:271–284.

Matsunaga TO, Sheeran PS, Luois S, Streeter JE, Mullin LB, Banerjee B, Dayton PA. Phase-change nanoparticles using highly volatile per-fluorocarbons: Toward a platform for extravascular ultrasound imaging. Theranostics 2012;2:1185–1198.

Overvelde MLJ, Garbin V, Sijl J, Dollet B, de Jong N, Lohse D, Versluis M. Nonlinear shell behavior of phospholipid-coated microbubbles. Ultrasound Med Biol 2010;36:2080–2092.

Phillips LC, Puett C, Sheeran PS, Dayton PA, Miller GW, Matsunaga TO. Phase-shift perfluorocarbon agents enhance high intensity focused ultrasound thermal delivery with reduced near-field heating. J Acoust Soc Am 2013;134:1473–1482.

Rapoport N. Phase-shift, stimuli-responsive perfluorocarbon nanodroplets for drug delivery to cancer. Wiley Interdiscip Rev Nanomed Nanobiotechnol 2012;4:492–510.

Reznik N, Seo M, Williams R, Bolewska-Pedyczak E, Lee M, Matsuura N, Gariepy J, Foster FS, Burns PN. Optical studies of vaporization and stability of fluorescently labelled perfluorocarbon droplets. Phys Med Biol 2012;57:7205–7217.

Reznik N, Shpak O, Gelderblom EC, Williams R, de Jong N, Versluis M, Burns PN. The efficiency and stability of bubble formation by acoustic vaporization of submicron perfluorocarbon droplets. Ultrasonics 2013;53:1368–1376.

Reznik N, Williams R, Burns PN. Investigation of vaporized submicron perfluorocarbon droplets as an ultrasound contrast agent. Ultrasound Med Biol 2011;37:1271–1279.

Schneider M. Characteristics of SonoVue ™. Echocardiogr-J Card 1999;16:743–746.

Sheeran PS, Matsunaga TO, Dayton PA. Phase-transition thresholds and vaporization phenomena for ultrasound phase-change nanoemulsions assessed via high-speed optical microscopy. Phys Med Biol 2013;58:4513–4534.

Sheeran PS, Wong VP, Luois S, McFarland RJ, Ross WD, Feingold S, Matsunaga TO, Dayton PA. Decafluorobutane as a phase-change contrast agent for low-energy extravascular ultrasonic imaging. Ultrasound Med Biol 2011;37:1518–1530.

Sheeran PS, Matsunaga TO, Dayton PA. Phase change events of volatile liquid perfluorocarbon contrast agents produce unique acoustic signatures. Phys Med Biol 2014;59:379–401.

Shpak O, Stricker L, Versluis M, Lohse D. The role of gas in ultrasonically driven vapor bubble growth. Phys Med Biol 2013a;58:2523–2535.

Shpak O, Kokhuis TJA, Luan Y, Lohse D, de Jong N, Fowlkes JB, Fabiilli M, Versluis M. Ultrafast dynamics of the acoustic vaporization of phase-change microdroplets. J Acoust Soc Am 2013b;134:1610–1621.

Sijl J, Overvelde MLJ, Dollet B, Garbin V, de Jong N, Lohse D, Versluis M. 'Compression-only' behavior: A second-order nonlinear response of ultrasound contrast agent microbubbles. J Acoust Soc Am 2011a;129:1729–1739.

Sijl J, Vos HJ, Rozendal T, de Jong N, Lohse D, Versluis M. Combined optical and acoustical detection of single microbubble dynamics. J Acoust Soc Am 2011b;130:3271–3281.

Simpson DH, Chin CT, Burns PN. Pulse inversion Doppler: A new method for detecting nonlinear echoes from microbubble contrast agents. IEEE Trans Ultrason Ferroelectr Freq Control 1999;46:372–382.

Tremblay-Darveau C, Williams R, Burns PN. Measuring absolute blood pressure using microbubbles. Ultrasound Med Biol 2014;40:775–787.

Van der Meer SM, Dollet B, Voormolen MM, Chin CT, Bouakaz A, de Jong N, Versluis M, Lohse D. Microbubble spectroscopy of ultrasound contrast agents. J Acoust Soc Am 2007;121:648–656.

Williams R, Wright C, Cherin E, Reznik N, Lee M, Gorelikov I, Foster FS, Matsuura N, Burns PN. Characterization of submicron phase-change perfluorocarbon droplets for extravascular ultrasound imaging of cancer. Ultrasound Med Biol 2013;39:475–489.